



**Providing Choice & Value**

Generic CT and MRI Contrast Agents



CONTACT REP

**AJNR**

**Optic Nerve Sheath MR Imaging  
Measurements in Patients with Orthostatic  
Headaches and Normal Findings on  
Conventional Imaging Predict the Presence of  
an Underlying CSF-Venous Fistula**

This information is current as  
of July 18, 2025.

Wouter I. Schievink, Marcel M. Maya, Angelique Sao-Mai  
S. Tay, Peyton L. Nisson, Jay Acharya, Rachelle B. Taché  
and Miriam Nuño

*AJNR Am J Neuroradiol* 2024, 45 (5) 655-661

doi: <https://doi.org/10.3174/ajnr.A8165>

<http://www.ajnr.org/content/45/5/655>

# Optic Nerve Sheath MR Imaging Measurements in Patients with Orthostatic Headaches and Normal Findings on Conventional Imaging Predict the Presence of an Underlying CSF-Venous Fistula

Wouter I. Schievink, Marcel M. Maya, Angelique Sao-Mai S. Tay, Peyton L. Nisson, Jay Acharya, Rachelle B. Taché, and Miriam Nuño



## ABSTRACT

**BACKGROUND AND PURPOSE:** Spontaneous spinal CSF leaks typically cause orthostatic headache, but their detection may require specialized and invasive spinal imaging. We undertook a study to determine the value of simple optic nerve sheath MR imaging measurements in predicting the likelihood of finding a CSF-venous fistula, a type of leak that cannot be detected with routine spine MR imaging or CT myelography, among patients with orthostatic headache and normal conventional brain and spine imaging findings.

**MATERIALS AND METHODS:** This cohort study included a consecutive group of patients with orthostatic headache and normal conventional brain and spine imaging findings who underwent digital subtraction myelography under general anesthesia to look for spinal CSF-venous fistulas.

**RESULTS:** The study group consisted of 93 patients (71 women and 22 men; mean age, 47.5 years; range, 17–84 years). Digital subtraction myelography demonstrated a CSF-venous fistula in 15 patients. The mean age of these 8 women and 7 men was 56 years (range, 23–83 years). The mean optic nerve sheath diameter was 4.0 mm, and the mean perioptic subarachnoid space was 0.5 mm in patients with a CSF-venous fistula compared with 4.9 and 1.2 mm, respectively, in patients without a fistula ( $P < .001$ ). Optimal cut-off values were found at 4.4 mm for optic nerve sheath diameter and 1.0 mm for the perioptic subarachnoid space. Fistulas were detected in about 50% of patients with optic nerve sheath diameter or perioptic subarachnoid space measurements below these cutoff values compared with <2% of patients with optic nerve sheath diameter or perioptic subarachnoid space measurements above these cutoff values. Following surgical ligation of the fistula, optic nerve sheath diameter increased from 4.0 to 5.3 mm and the perioptic subarachnoid space increased from 0.5 to 1.2 mm ( $P < .001$ ).

**CONCLUSIONS:** Concerns about a spinal CSF leak should not be dismissed in patients with orthostatic headache when conventional imaging findings are normal, and simple optic nerve sheath MR imaging measurements can help decide if more imaging needs to be performed in this patient population.

**ABBREVIATIONS:** BMI = body mass index; DSM = digital subtraction myelography; ONS = optic nerve sheath; ONSD = optic nerve sheath diameter; OP = opening pressure; SAS = subarachnoid space; SIHDAS = SIH Disability Assessment Score; SIH = spontaneous intracranial hypotension

Orthostatic headaches, ie, headaches that worsen after assuming the upright position and that are least noticeable on awakening in the morning before getting out of bed, are the hallmark of spontaneous intracranial hypotension (SIH).<sup>1,2</sup> CSF leaks

at the level of the spine are responsible for causing SIH in most patients.<sup>1</sup>

The diagnosis of SIH can be made with confidence under the following circumstances: 1) brain MR imaging shows a combination of  $\geq 1$  of the typical reversible findings of SIH, ie, subdural fluid collections, enhancement of the pachymeninges, engorgement of venous structures, pituitary enlargement, and sagging of the brain (mnemonic, SEEPS); or 2) if spine imaging shows the presence of an extradural CSF collection, indicating a dural tear and CSF leak.<sup>1,3</sup> An estimated one-fifth of patients with spinal CSF leaks have normal findings on brain imaging.<sup>4</sup> However, a common type of spontaneous spinal CSF leak, the CSF-venous fistula, is not associated with an extradural spinal CSF collection

Received October 17, 2023; accepted after revision January 4, 2024.

From the Departments of Neurosurgery (W.I.S., A.S.-M.S.T., P.L.N., R.B.T.) and Imaging (M.M.M., J.A.), Cedars-Sinai Medical Center, Los Angeles, California; and Department of Public Health Sciences (M.N.), University of California, Davis, Davis, California.

Please address correspondence to Wouter I. Schievink, MD, Department of Neurosurgery, Cedars-Sinai Medical Center, 127 South San Vicente Blvd, Los Angeles, CA 90048; e-mail: schievinkw@cshs.org; @WouterSchievink

Indicates article with online supplemental data.

<http://dx.doi.org/10.3174/ajnr.A8165>

and thus is not detectable on routine CT myelography or spine MR imaging.<sup>1</sup> These spinal CSF-venous fistulas require specialized imaging with digital subtraction myelography (DSM)<sup>5,6</sup> or dynamic CT myelography<sup>6,7</sup> for their detection. In a prior study using DSM, we found that approximately 10% of patients with orthostatic headaches and normal conventional brain and spine imaging findings have an underlying spinal CSF-venous fistula.<sup>8</sup> Since the completion of that study, we have added MR imaging sequences to our SIH protocol that allow precise measurements of the optic nerve sheath (ONS). The ONS diameter (ONSD) is correlated with CSF pressure and is known to be significantly altered in not only intracranial hypertension but also SIH.<sup>9-14</sup> However, to our knowledge, the ONSD has not been studied in patients with orthostatic headaches and normal findings on routine brain and spine imaging. The hypothesis of the current study is that ONSD could be affected by the presence of a CSF-venous fistula causing loss of CSF in the setting of otherwise normal brain MR imaging findings.

## MATERIALS AND METHODS

This cohort study was approved by the Cedars-Sinai Medical Center institutional review board, who waived the requirement for written informed consent.

The patient population consisted of a consecutive group of patients with orthostatic headaches, normal findings on brain MR imaging, and no evidence of extradural CSF on spine MR imaging with MR myelography,<sup>15</sup> who underwent DSM in the lateral decubitus position between June 2020 and May 2022. The goal of DSM was to identify a spontaneous spinal CSF-venous fistula. Patients who had a history of any prior brain MR imaging or spinal imaging consistent with SIH or spinal CSF leak and patients who did not have a brain MR imaging performed at our institution with the SIH protocol before DSM were excluded from the analysis.

### SIH Disability Assessment Score

All patients completed a modified Migraine Disability Assessment Test 5-item questionnaire to assess the severity of the symptoms before and after treatment.<sup>16</sup> This questionnaire measures disability in 3 domains of activity (employment, household work, and nonwork activities), capturing the number of days affected during a 3-month period, with the score ranging from 0 to 270 (3 [domains] × 3 [months] × 30 [days]).<sup>16</sup> The modification consists of substituting “symptoms of SIH” for “headaches.” We refer to this modified questionnaire as the SIH Disability Assessment Score questionnaire. (SIHDAS).<sup>17</sup> A score of 0–5 (grade I) equates to little or no disability, a score of 6–10 (grade II) is mild disability, a score of 11–20 (grade III) is moderate disability, and a score of 21–270 (grade IV) is severe disability.

### Brain MR Imaging Protocol

MR imaging was performed on 1.5 or 3T scanners. The SIH brain MR imaging protocol is shown in the Online Supplemental Data. The MR imaging sequences allowing precise measurements of the ONS consisted of coronal fat-suppressed T2-weighted sequences through the orbit (TR = 5750 ms, TE = 99 ms, flip angle = 150°, section thickness = 3.0 mm, section gap = 0%, FOV = 230 mm<sup>2</sup>).

### Definition of Normal Brain MR Imaging Findings

The findings of a normal brain MR imaging were based on the report of 1 of 4 board-certified neuroradiologists, all with a special interest in SIH. For this study, findings of all brain MR imaging designated as normal were re-reviewed by 1 board-certified neuroradiologist who was not involved in the initial interpretation of the brain MR imaging and 1 board-certified neurosurgeon to confirm the absence of the reversible findings of SIH, ie, subdural fluid collections; enhancement and/or thickening of the pachymeninges; venous engorgement using the venous distention sign;<sup>18</sup> pituitary enlargement using the measurements of maximal pituitary height;<sup>19</sup> and brain sagging using a cutoff of 5.5 mm for the pontomammillary distance,<sup>20</sup> a cutoff of 45° for the pontomesencephalic angle,<sup>21</sup> and a cutoff of 5 mm for cerebellar tonsillar herniation. In addition, the absence of infratentorial superficial siderosis<sup>22</sup> and calvarial hyperostosis,<sup>23</sup> the 2 mostly irreversible brain MR imaging findings that may be observed in patients with chronic SIH, was confirmed. Any discrepancies were adjudicated by a second board-certified neuroradiologist.

### Brain MR Imaging Assessments

The ONSD and perioptic subarachnoid space (Fig 1) were measured by 2 board-certified neuroradiologists and 1 senior neurosurgery resident blinded to the outcome of the DSM. On the basis of prior measurements of ONSD and perioptic subarachnoid space as reported by Rohr et al,<sup>24</sup> who found significant variability of these measurements within the first 10 mm of the optic nerve, measurements were made 10–12 mm posterior to the globe. In addition, a previously published and validated probabilistic score for the presence of SIH, known as the Bern score,<sup>25</sup> was calculated by the same 2 board-certified neuroradiologists and a senior neurosurgery resident blinded to the outcome of the DSM. Measurements by an individual physician of the ONSD, perioptic subarachnoid space, and Bern score were averaged for the final measurement.

### DSM Technique

In all patients, the DSM technique as described by Hoxworth et al<sup>26</sup> was used with some minor modifications.<sup>5,27</sup> Briefly, DSM is performed with the patient under general endotracheal anesthesia with deep paralysis and suspended respiration for maximal detail and temporal resolution. Patients are positioned in the lateral decubitus position in a biplane angiography suite, with tilt table capability. Pillows or foam padding are placed to optimize cervicothoracic alignment. Under fluoroscopic guidance, a 22-ga needle is placed midline, usually at the L2–3 level, being careful to avoid tenting and subdural injection. An opening pressure is obtained at this time. Then, an accurate needle position is confirmed with an injection of 0.5 mL of contrast (Omnipaque 240 or 300 mg/mL; GE Healthcare). Patients are then further positioned on the basis of the area of interest, with the table tilted to achieve contrast flow to the cervicothoracic spine. Finally, contrast is injected manually 1 mL per second, with suspended respiration for 60–75 seconds while acquiring biplane subtraction images at 1–2 frames per second.

### Statistical Analysis

Continuous variables are presented as means (SDs) in addition to medians and interquartile ranges. Categorical variables are presented

as absolute numbers and percentages. Comparison of demographic and disease characteristics between groups by fistula status are performed using a *t* test or Mann-Whitney Wilcoxon test for continuous variables, and  $\chi^2$  and Fisher exact tests are performed to compare categorical variables. Logistic regression analysis was used to calculate the predicted probability of a fistula. Receiver operating

characteristic curves were used to determine optimal thresholds for perioptic subarachnoid space and the ONSD for the outcome of a fistula. We computed agreement ( $\kappa$ ) of the perioptic subarachnoid space, ONSD, and Bern scores among multiple raters implementing the Magree macro (<https://www.agreestat.com/books/sas2/chap3/chap3sas.pdf>) in the subarachnoid space (SAS). Pearson

correlation coefficients were calculated among body mass index (BMI), opening pressure (OP), ONSD, and the perioptic subarachnoid space. All statistical analyses were performed using SAS, Version 9.4 (SAS Institute).

## RESULTS

### Clinical and Radiographic Characteristics

The mean age of the 93 patients with orthostatic headache was 47.5 (SD, 15.7) years. There were 71 women (76.3%) and 22 men (23.7%). The mean duration of orthostatic headache was 51.2 months (median, 32 months). An occipital or suboccipital headache was the most common, occurring in 43 patients (46.2%). At the onset of symptoms, orthostatic worsening of the headache occurred within 10 minutes in 35 patients (37.6%), between 11 and 60 minutes in 32 patients (34.4%), and after 60 minutes in 26 patients (31.2%).

Lateral decubitus DSM demonstrated a CSF-venous fistula in 15 (16.1%) of the 93 patients. The mean age of the 7 men and 8 women was 56 (14.4 SD) years. There was a less pronounced female preponderance among the patients with

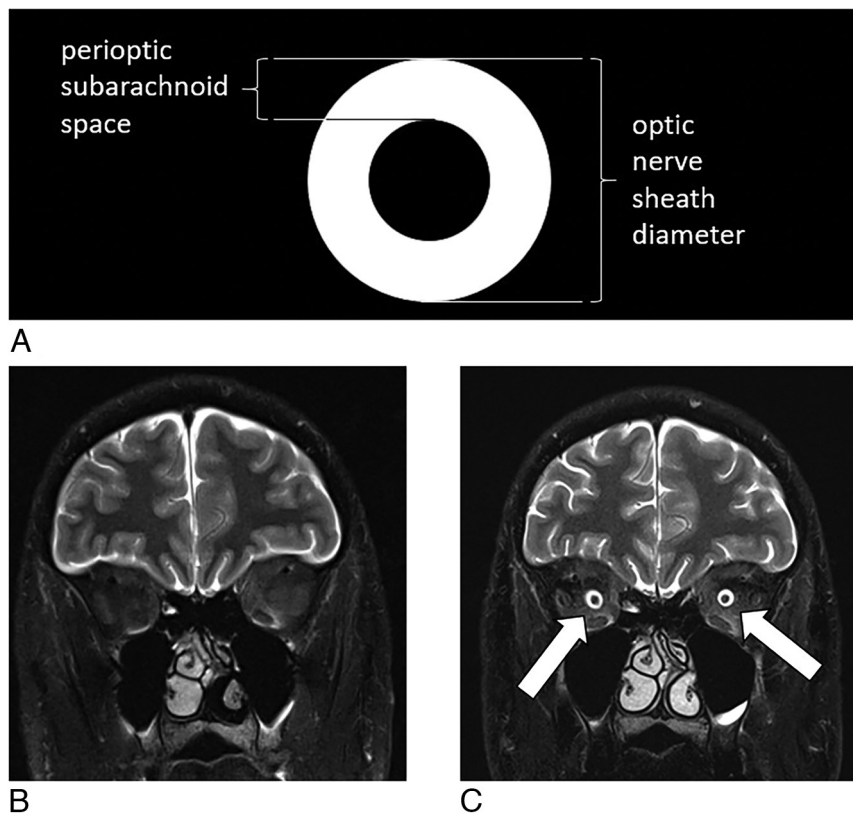


**FIG 1.** How to measure the ONSD and perioptic subarachnoid space. Illustration (A) depicting the measurements for the ONSD and the perioptic subarachnoid space. Pre- (B) and post- (C) operative coronal fat-suppressed T2-weighted MR imaging shows restoration of the perioptic subarachnoid space (arrows) following ligation of a spinal CSF-venous fistula.

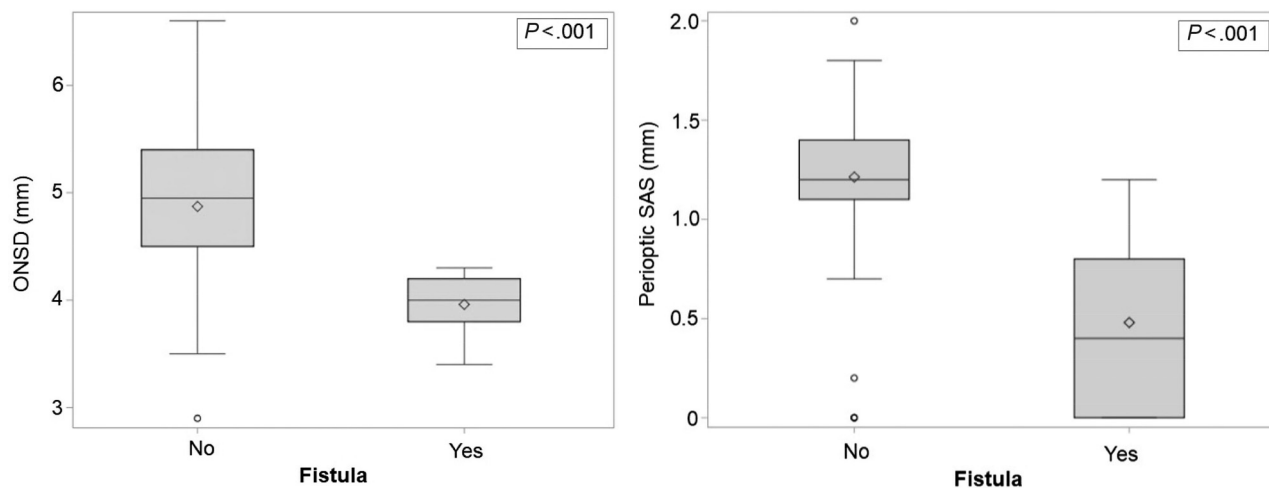


**FIG 2.** ONSD and perioptic subarachnoid space measurements in patients with and without spinal CSF-venous fistulas. Box and whisker plots of the ONSD and perioptic SAS in patients without and with a spinal CSF-venous fistula. The box represents the upper and lower quartiles with the line splitting the box representing the median. The diamond represents the mean. The whiskers represent the upper and lower values of the data, up to 1.5 times the interquartile range. The single points represent the outliers.

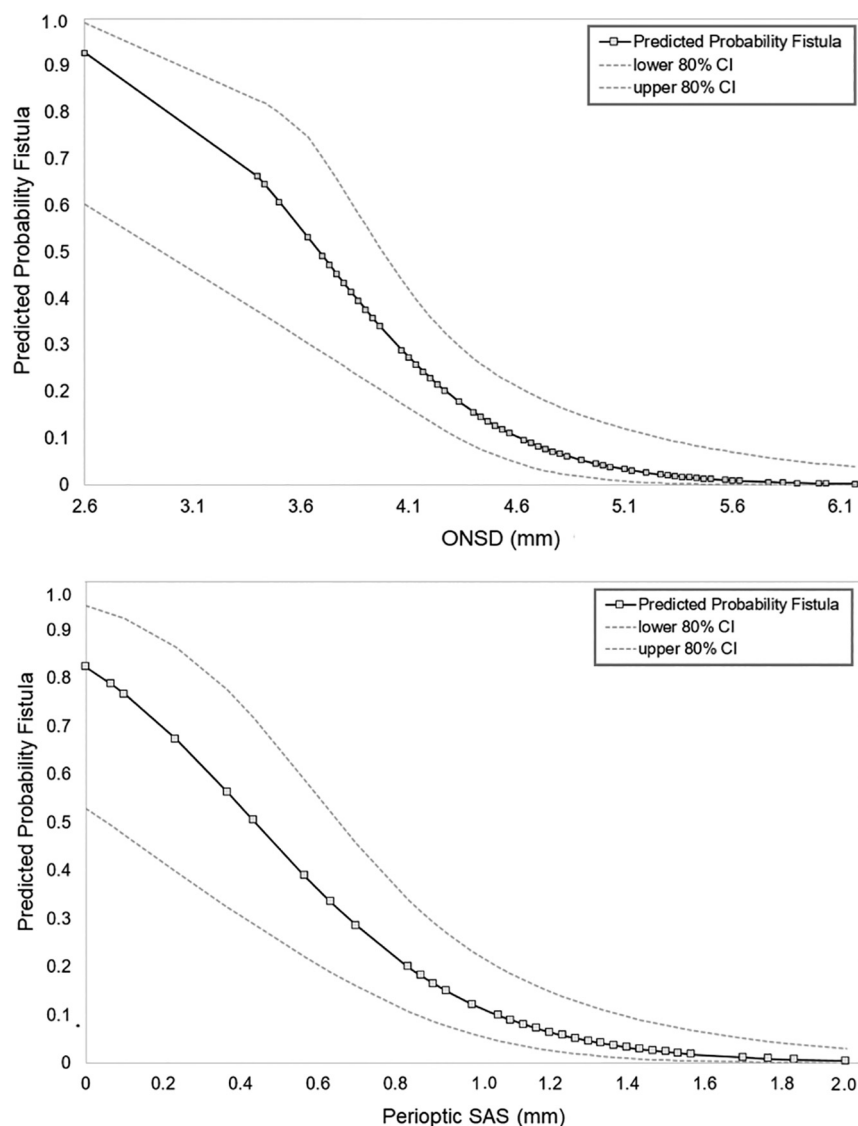


**FIG 3.** Predicted probability of finding a spinal CSF-venous fistula based on the ONSD and perioptic subarachnoid space measurements. The graphs depict the predicted probability (and 80% confidence intervals) of identifying a CSF-venous fistula according to ONSD and perioptic SAS.

a CSF-venous fistula ( $P = .022$ ), and these patients were about a decade older than patients without a CSF-venous fistula ( $P = .015$ ), but there were no significant differences in the duration of symptoms, location of the headache, time to orthostatic worsening of the headache, BMI, results of prior epidural blood patching, time interval between the onset of symptoms and the first brain MR imaging, or time interval between the brain MR imaging with the SIH protocol and DSM (Online Supplemental Data). Although CSF opening pressure was normal in all patients (reference range, 6–25 cm CSF), it was lower in those who were found to have a CSF-venous fistula (13.3 versus 16.1 cm CSF;  $P < .016$ ). A CSF-venous fistula was found in 19.4% of patients with a spinal meningeal diverticulum and in 4.8% of those without such a diverticulum ( $P = .177$ ). The SIHDAS was II in 1 patient, III in 1 patient, and IV in 13 patients. All 15 patients had a single CSF-venous fistula, and all fistulas were located in the thoracic spine. The CSF-venous fistula was on the right side in 9 patients and on the left side in 6 patients.

cutoff point of 4.4 mm for identifying a CSF-venous fistula, specificity was 79.5% and sensitivity was 100%. With the perioptic subarachnoid space cutoff point of 1.0 mm for identifying a CSF-venous fistula, specificity was 85.9% and sensitivity was 93.3%.

There was no significant difference in the mean Bern score between patients with a CSF-venous fistula (0.58) compared with those without a CSF-venous fistula (0.64) ( $P = .78$ ). Interrater agreement was substantial for all measurements, including the Bern score ( $\kappa = 0.73$ ), perioptic subarachnoid space ( $\kappa = 0.79$ ), and the ONSD ( $\kappa = 0.87$ ). Significant linear correlations were found between the ONSD and the perioptic subarachnoid space with CSF opening pressure and BMI (Fig 4).

#### **Treatment of a Spinal CSF-Venous Fistula and the Postoperative Course**

All 15 patients with a CSF-venous fistula underwent an uneventful laminoforaminotomy for clip ligation of the fistula. Postoperative brain MR imaging with the same SIH protocol was performed in

#### **Findings among Those with and without a Spinal CSF-Venous Fistula**

The mean ONSD was significantly decreased in patients with a CSF-venous fistula (4.0 mm), compared with patients without a CSF-venous fistula (4.9 mm) ( $P < .001$ ) (Fig 2). This difference in the ONSD was mostly due to the reduction of the perioptic subarachnoid space, a component of the ONSD. The mean perioptic subarachnoid space measured 0.5 mm among the patients with a CSF-venous fistula and 1.2 mm in the patients without a CSF-venous fistula ( $P < .001$ ) (Fig 2). By means of the Youden index analysis, optimal cutoff values were found at 4.4 mm for ONSD and 1.0 mm for the perioptic subarachnoid space. Using these cutoff values, we detected fistulas in 47% and 54% of patients, respectively, with the ONSD or perioptic subarachnoid space measurements below these cutoff values compared with 0% and 2% of patients with ONSD or perioptic subarachnoid space measurements above these cutoff values. The predicted probability of identifying a CSF-venous fistula increased  $<1\%$  at a perioptic subarachnoid space of 1.8 mm to 82% at a perioptic subarachnoid space of 0 mm, and from  $<1\%$  at an ONSD of 5.7 mm to 93% at an ONSD of 2.6 mm (Fig 3).

Receiver operating characteristic curve analysis revealed an area under the curve of 0.883 (95% CI, 0.816–0.950) for ONSD and 0.932 (95% CI, 0.877–0.987) for the perioptic subarachnoid space. By means of the ONSD



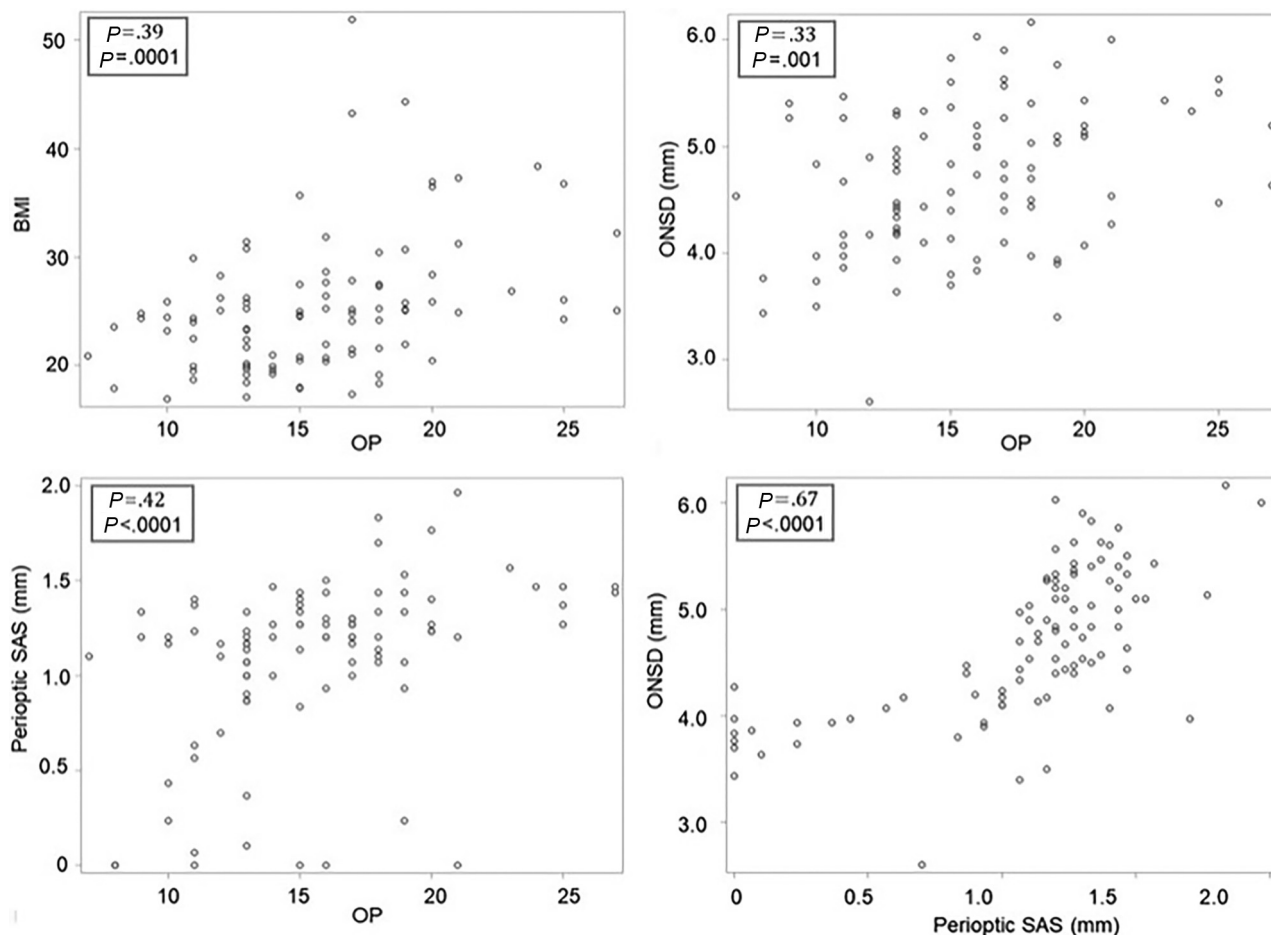


**FIG 4.** The relationship among the BMI, CSF opening pressure, ONSD, and perioptic subarachnoid space. Scatterplots depict the relationships among BMI, CSF OP (in centimeters CSF), ONSD, and the perioptic SAS. By ranking from the weakest to the strongest correlation, positive correlations are found between the ONSD and OP, BMI and OP, perioptic SAS and OP, and ONSD and perioptic SAS.

14 of the 15 patients between 18 and 52 hours (mean, 40 hours) following surgical ligation of the CSF-venous fistula. Postoperatively, the ONSD increased from 4.0 to 5.3 mm, and the perioptic subarachnoid space increased from 0.5 to 1.2 mm ( $P < .001$ ) (Fig 5). There was no change in the Bern score (0.58 to 0.42). During a mean clinical postoperative follow-up of 10 months (range, 3–26 months), 12 patients (80%) reported complete or near-complete and sustained resolution of SIH symptoms (SIHDAS grade II, III, or IV to grade I), 1 patient (6.7%) reported incomplete resolution of SIH symptoms (SIHDAS grade IV to III), and 2 patients (13.3%) reported no change in SIH symptoms (SIHDAS grade IV). The mean SIHDAS for all 15 patients improved from 139.9 to 21.5 ( $P < .001$ ).

## DISCUSSION

In this study, we found that among patients with orthostatic headache and normal findings on conventional brain and spine imaging, the ONSD and perioptic subarachnoid space were significantly decreased in patients with a CSF-venous fistula compared with patients without a CSF-venous fistula. In this patient population, we found CSF-venous fistulas in about one-half of patients with a perioptic subarachnoid space measuring  $\leq 1.0$  mm or with an ONSD measuring  $\leq 4.4$  mm (measured 10–12 mm posterior to the globe) compared with  $< 2\%$  of patients with measurements above these cutoff values.

The perioptic subarachnoid space is a continuation of the intracranial subarachnoid space, and unlike the intracranial subarachnoid space that is enveloped by the dura mater, it is surrounded by the soft tissues of the orbit, allowing unrestricted expansion or collapse depending on the amount of CSF volume.<sup>28,29</sup> We hypothesize that in the presently reported patients with CSF-venous fistulas and normal findings on conventional brain MR imaging, the CSF loss was sufficient to cause a decrease in the perioptic subarachnoid space volume but not sufficient to cause the other brain MR imaging features of SIH. Rapid restoration of the normal perioptic subarachnoid space was seen within about 24–48 hours after surgical ligation of the CSF-venous fistula. In a series of experiments, Hansen and Helmke<sup>30</sup> have shown a prompt response of the ONS to changes in spinal CSF volume and pressure.

In our prior study, we found CSF-venous fistulas in 10% of patients with orthostatic headache but normal conventional brain and spine imaging findings; fistulas were present in 20% of patients with meningeal diverticula and in none of the patients without diverticula.<sup>8</sup> Although we found similar results in the current study, the number of patients without meningeal diverticula was relatively small and the difference did not reach statistical significance. Prior studies have shown a relationship between the ONSD and BMI and between the ONSD and CSF pressure. The ONSD is weakly correlated with BMI and strongly

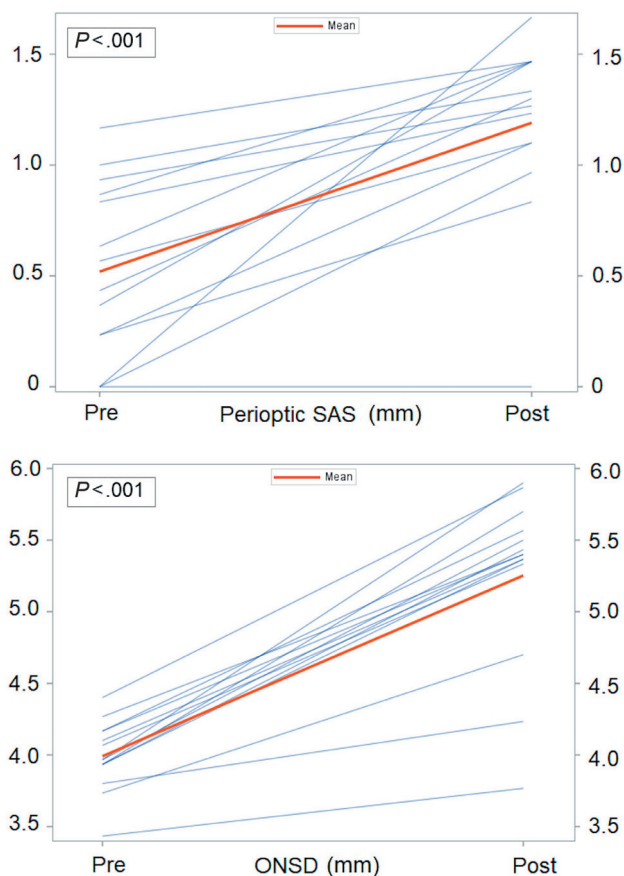


**FIG 5.** Normalization of the ONSD and perioptic subarachnoid space following ligation of spinal CSF-venous fistulas. Individual measurements of the pre- and postoperative ONSD and perioptic SAS following ligation of the spinal CSF-venous fistula.

correlated with CSF opening pressure and with intracranial pressure. We were able to replicate these findings for BMI, ONSD, and CSF opening pressure, providing internal validation of the data.

The Bern score is based on a summation of several of the well-established features of SIH on brain MR imaging and was established and validated to predict the presence of spinal extradural CSF and specifically excluded CSF-venous fistulas,<sup>25</sup> but subsequently, this score has also been used in the evaluation and follow-up of patients with SIH due to CSF-venous fistulas.<sup>31</sup> In the present study of patients with orthostatic headaches and normal conventional brain and spine imaging findings, the Bern score was not able to differentiate patients with a CSF-venous fistula from those without such a fistula, and there was no change in the Bern score following surgical ligation of the CSF-venous fistula.

The MR imaging sequence used in the present study adds 4 minutes of MR imaging time. This MR imaging sequence allows precise and reproducible measurements, and in our study, interrater agreement was substantial for both the perioptic subarachnoid space and the ONSD. Ultrasonography also has been used extensively for the evaluation of the ONS and has the advantage of obtaining measurements in different body positions, but the technology is very user-dependent, limiting its use.<sup>12,14</sup>

The burden of SIH is high among patients seeking medical care,<sup>32-34</sup> and this was reflected in the SIHDAS in the present study, showing severe disability in almost all patients. Following treatment of the CSF-venous fistula, the SIHDAS was significantly improved with complete or near-complete resolution of the symptoms of SIH in 80% of patients.

It has been known since the 1990s that CSF opening pressure may be normal in patients with SIH,<sup>35</sup> and this finding has now been confirmed in several SIH patient populations, including in patients with CSF-venous fistulas.<sup>5,8,36</sup> In the current study, all patients had a normal CSF opening pressure, but CSF opening pressure was lower in those with a CSF-venous fistula.

Spontaneous spinal CSF-venous fistulas were first described in 1914.<sup>37</sup> These abnormal communications between the spinal subarachnoid space and epidural veins were initially believed to be rare but are now known to be a common cause of SIH. The radiographic studies necessary for the reliable detection of CSF-venous fistulas currently require a lumbar puncture and use an iodine-based contrast agent and ionizing radiation, are expensive and time-consuming, and, in our institution, are performed with the patient under general endotracheal anesthesia. The current study shows that measurements of the ONSD and perioptic subarachnoid space will be of use in making decisions regarding increasing imaging for patients with orthostatic headache but otherwise normal conventional brain and spine imaging findings.

This study had some limitations. First, the current study mostly represents a highly selected group of patients referred to a quaternary referral center for SIH, and the generalizability of our findings is unknown. However, the radiographic techniques capable of reliably demonstrating spinal CSF-venous fistulas are not widely available and are mainly used in high-volume SIH referral centers. Second, this study was undertaken during the coronavirus 2019 (COVID-19) pandemic, and this timing may have introduced referral and other biases favoring a patient population with higher disability. However, the overall detection rate of finding a CSF-venous fistula was very similar to that in a prior study performed before the COVID-19 pandemic. Third, brain MR imaging findings of SIH may spontaneously resolve with time despite persistent symptoms, and the timing of MR imaging in our study could not be standardized. However, the time interval between the onset of symptoms and the first MR imaging did not differ between those with and without a CSF-venous fistula. Finally, this was a single-center study, and the relatively small number of patients resulted in our calculations having relatively wide confidence intervals.

## CONCLUSIONS

ONS MR imaging measurements showing a reduced ONS diameter and perioptic subarachnoid space predict the presence of an underlying spinal CSF-venous fistula in patients with orthostatic headaches and normal conventional brain and spine imaging findings. In addition, ONS measurements normalized promptly after ligation of the fistula.

**Disclosure forms** provided by the authors are available with the full text and PDF of this article at [www.ajnr.org](http://www.ajnr.org).

## REFERENCES

- Schievink WI. Spontaneous intracranial hypotension. *N Engl J Med* 2021;385:2173–78 [CrossRef Medline](#)
- Mehta D, Cheema S, Davagnanam I, et al. Diagnosis and treatment evaluation in patients with spontaneous intracranial hypotension. *Front Neurol* 2023;14:1145949 [CrossRef Medline](#)
- Schievink WI. Spontaneous spinal cerebrospinal fluid leaks and intracranial hypotension. *JAMA* 2006;295:2286–96 [CrossRef Medline](#)
- D'Antona L, Jaime Merchan MA, Vassiliou A, et al. Clinical presentation, investigation findings, and treatment outcomes of spontaneous intracranial hypotension syndrome: a systematic review and meta-analysis. *JAMA Neurol* 2021;78:329–37 [CrossRef Medline](#)
- Schievink WI, Maya MM, Moser FG, et al. Lateral decubitus digital subtraction myelography to identify spinal CSF-venous fistulas in spontaneous intracranial hypotension. *J Neurosurg Spine* 2019;31:1–4 [CrossRef Medline](#)
- Kranz PG, Gray L, Malinzak MD, et al. CSF-venous fistulas: anatomy and diagnostic imaging. *AJR Am J Roentgenol* 2021;217:1418–29 [CrossRef Medline](#)
- Mamlouk MD, Ochi RP, Jun P, et al. Decubitus CT myelography for CSF-venous fistulas: a procedural approach. *AJNR Am J Neuroradiol* 2021;42:32–36 [CrossRef Medline](#)
- Schievink WI, Maya M, Prasad RS, et al. Spontaneous spinal cerebrospinal fluid-venous fistulas in patients with orthostatic headaches and normal conventional brain and spine imaging. *Headache* 2021;61:387–91 [CrossRef Medline](#)
- Watanabe A, Horikoshi T, Uchida M, et al. Decreased diameter of the optic nerve sheath associated with CSF hypovolemia. *AJNR Am J Neuroradiol* 2008;29:863–64 [CrossRef Medline](#)
- Rohr A, Jensen U, Riedel C, et al. MR imaging of the optic nerve sheath in patients with craniocervical hypotension. *AJNR Am J Neuroradiol* 2010;31:1752–57 [CrossRef Medline](#)
- Takeuchi N, Horikoshi T, Kinouchi H, et al. Diagnostic value of the optic nerve sheath subarachnoid space in patients with intracranial hypotension syndrome. *J Neurosurg* 2012;117:372–77 [CrossRef Medline](#)
- Fichtner J, Ulrich CT, Fung C, et al. Management of spontaneous intracranial hypotension: transorbital ultrasound as discriminator. *J Neurol Neurosurg Psychiatry* 2016;87:650–55 [CrossRef Medline](#)
- Holbrook JF, Hudgins PA, Bruce BB, et al. Novel orbital findings of intracranial hypotension. *Clin Imaging* 2017;41:125–31 [CrossRef Medline](#)
- Wang L-J, Zhang Y, Li C, et al. Ultrasonographic optic nerve sheath diameter as a noninvasive marker for intracranial hypotension. *Ther Adv Neurol Disord* 2022;15:17562864211069744 [CrossRef Medline](#)
- Tay ASS, Maya M, Moser FG, et al. Computed tomography vs heavily T2-weighted magnetic resonance myelography for the initial evaluation of patients with spontaneous intracranial hypotension. *JAMA Neurol* 2021;78:1275–76 [CrossRef Medline](#)
- Stewart WF, Lipton RB, Whyte J, et al. An international study to assess reliability of the Migraine Disability Assessment (MIDAS) score. *Neurology* 1999;53:988–94 [CrossRef Medline](#)
- Schievink WI, Maya MM, Barnard ZR, et al. Behavioral variant frontotemporal dementia as a serious complication of spontaneous intracranial hypotension. *Oper Neurosurg (Hagerstown)* 2018;15:505–15 [CrossRef Medline](#)
- Farb RI, Forghani R, Lee SK, et al. The venous distension sign: a diagnostic sign of intracranial hypotension at MR imaging of the brain. *AJNR Am J Neuroradiol* 2007;28:1489–93 [CrossRef Medline](#)
- Forghani R, Farb RI. Diagnosis and temporal evolution of signs of intracranial hypotension on MRI of the brain. *Neuroradiology* 2008;50:1025–34 [CrossRef Medline](#)
- Shah LM, McLean LA, Heilbrun ME, et al. Intracranial hypotension: improved MRI detection with diagnostic intracranial angles. *AJR Am J Roentgenol* 2013;200:400–07 [CrossRef Medline](#)
- Houk JL, Amrhein TJ, Gray L, et al. Differentiation of Chiari malformation type I and spontaneous intracranial hypotension using objective measurements of midbrain sagging. *J Neurosurg* 2021;136:1796–803 [CrossRef Medline](#)
- Schievink WI, Maya MM, Harris J, et al. Infratentorial superficial siderosis and spontaneous intracranial hypotension. *Ann Neurol* 2023;93:64–75 [CrossRef Medline](#)
- Johnson DR, Carr CM, Luetmer PH, et al. Diffuse calvarial hyperostosis in patients with spontaneous intracranial hypotension. *World Neurosurg* 2021;146:e848–53 [CrossRef Medline](#)
- Rohr A, Riedel C, Reimann G, et al. Pseudotumor cerebri: quantitative normalwerte anatomischer kennstrukturen im kraniellen MRT. *RoFo* 2008;180:884–90 [CrossRef Medline](#)
- Dobrocky T, Grunder L, Breiding PS, et al. Assessing spinal cerebrospinal fluid leaks in spontaneous intracranial hypotension with a scoring system based on brain magnetic resonance imaging findings. *JAMA Neurol* 2019;76:580–87 [CrossRef Medline](#)
- Hoxworth JM, Patel AC, Bosch EP, et al. Localization of a rapid CSF leak with digital subtraction myelography. *AJNR Am J Neuroradiol* 2009;30:516–19 [CrossRef Medline](#)
- Galvan J, Maya M, Prasad RS, et al. Spinal cerebrospinal fluid leak localization with digital subtraction myelography: tips, tricks, and pitfalls. *Radiol Clin* 2024;62:321–32 [CrossRef Medline](#)
- Anderson DR. Ultrastructure of meningeal sheaths: normal human and monkey optic nerves. *Arch Ophthalmol* 1969;82:659–74 [CrossRef Medline](#)
- Hayreh SS. The sheath of the optic nerve. *Ophthalmologica* 1984;189:54–63 [CrossRef Medline](#)
- Hansen HC, Helmke K. Validation of the optic nerve sheath response to changing cerebrospinal fluid pressure: ultrasound findings during intrathecal infusion tests. *J Neurosurg* 1997;87:34–40 [CrossRef Medline](#)
- Brinjikji W, Garza I, Whealy M, et al. Clinical and imaging outcomes of cerebrospinal fluid-venous fistula embolization. *J Neurointerv Surg* 2022;14:953–56 [CrossRef Medline](#)
- Cheema S, Joy C, Pople J, et al. Patient experience of diagnosis and management of spontaneous intracranial hypotension: a cross-sectional online survey. *BMJ Open* 2022;12:e057438 [CrossRef Medline](#)
- Jesse CM, Häni L, Fung C, et al. The impact of spontaneous intracranial hypotension on social life and health-related quality of life. *J Neurol* 2022;269:5466–73 [CrossRef Medline](#)
- Liaw V, McCreary M, Friedman DI. Quality of life in patients with confirmed and suspected spinal CSF leaks. *Neurology* 2023;101:e2411–22 [CrossRef Medline](#)
- Mokri B, Hunter SF, Atkinson JLD, et al. Orthostatic headaches caused by CSF leak but with normal CSF pressures. *Neurology* 1998;51:786–90 [CrossRef Medline](#)
- Kranz PG, Tanpitukpongse TP, Choudhury KR, et al. How common is normal cerebrospinal fluid pressure in spontaneous intracranial hypotension? *Cephalalgia* 2016;36:1209–17 [CrossRef Medline](#)
- Schievink WI, Moser FG, Maya MM. CSF-venous fistula in spontaneous intracranial hypotension. *Neurology* 2014;83:472–73 [CrossRef Medline](#)